npj | materials degradation

Article

Published in partnership with CSCP and USTB

https://doi.org/10.1038/s41529-024-00512-3

Dependency of tensile properties and biodegradation on molecular mass during hydrolysis of poly(butylene succinate)

Felix Eckel, Daniel Van Opdenbosch, Katharina Sophie Schandl & Cordt Zollfrank

The molecular mass of biodegradable polymers often explains the varying biodegradation results in outdoor environments and determines the mechanical properties and embrittlement of polymer samples. Accordingly, we have investigated the relationship between the molecular mass of poly(butylene succinate) (PBS) and its tensile properties and mineralisation. With decreasing molecular mass, we found that Young's modulus was rising while tensile strength and elongation at break were decreasing. A ductile-brittle transition was found between a M_w of 80,000 g/mol and 110,000 g/mol. The dependency of mechanical properties on molecular mass as determined after hydrolysis differed significantly from a study performed on freshly synthesised PBS. Biodegradation to CO_2 by microorganisms in a mixture of field soil and compost soil was found to begin at a M_w between 8060 g/mol and 26,666 g/mol. These results are essential for estimating the service life of products made from PBS.

The market value of poly(butylene succinate) (PBS) is estimated to have been USD 71.23 billion in 2021. PBS is expected to be increasingly used for packaging, agriculture, and biomedical applications, with a forecasted market value of USD 124.69 billion by 2029[1–3]. Polyester-based products like those made from PBS will degrade if placed in humid environments in which they are hydrolysed and will finally be completely mineralised to CO_2, water, and biomass[4]. Their mechanical properties are expected to change drastically during degradation from a polymer with a high molecular mass to lower molecular masses and, finally, monomers and small volatile compounds. Even for non-biodegradable polymers, the dependency of mechanical properties on the molecular mass changes or aging processes is important for determining the estimated lifetime, shelf life, and remaining service life of products in use. It is also essential during the selection of raw material, recycling, and estimating the fate of biopolymer particles and microplastic in the environment[5,6]. Much interest is taken in biomedical applications for which balancing mechanical properties and stability with the degradation of biodegradable bone implants, and tissue is helpful to enable a gradual load transfer to the regenerated structure[7–11]. This shows that for products that are degraded during their application, it is crucial to estimate how their mechanical properties and biodegradability change during the degradation process. Also, if the relationship between molecular mass, mechanical properties, and biodegradability is known, it would be possible to tailor the properties of a product according to its application by adjusting the molecular mass through hydrolysis. The mechanical properties depending on molecular mass changes or other aging processes have been investigated during photodegradation, thermal degradation, oxidative degradation, hydrolysis, and other degradation pathways on well-established polymers like polypropylene (PP), polyethylene (PE), poly(vinyl chloride) (PVC), poly(ethylene terephthalate) (PET), polyamides (PA) and polystyrene (PS)[5,6,12–23]. The biodegradation and its effect on mechanical properties of poly(lactic acid) (PLA) has been extensively studied[9,24–30]. Despite its economic value and scope of applications, few studies have been published on the relationship between mechanical properties and the molecular mass of PBS[31–33]. Not only are the mechanical properties expected to change with further hydrolysis, but biodegradability may also change. The biodegradation process can consist of several mechanisms. Ultimately, biodegradation means the complete mineralisation of the polymer to CO_2, water, and biomass under aerobic conditions and, additionally, methane under anaerobic conditions by microorganisms. Direct digestion by microorganisms is usually not possible due to the lack of water solubility and the considerable chain length of polymers[34]. Therefore, the rate-limiting step for biodegradation is usually the abiotic chemical hydrolysis for polyesters and can be accompanied by enzymatic hydrolysis in some environments due to excreted enzymes or by photodegradation[34–37].

The results of biodegradation studies vary widely, and the reason is often not clear[38–41]. In one study of PBS degradation in soil at 19 different sites, weight loss varied between 1.6% and 100%, with an average of 34.2 ± 36.2% after 12 months[39]. Therefore, identifying and quantifying

Chair for Biogenic Polymers, TUM Campus Straubing for Biotechnology and Sustainability, Technical University of Munich, Schulgasse 16, Straubing, 94315, Germany. e-mail: cordt.zollfrank@tum.de

factors affecting the biodegradation is of great interest. Environmental and sample parameters are influencing the biodegradation process. Usually, the most important factors regarding the sample are the polymer composition, the molecular mass of the polymer, and the crystallinity[31,42–46]. The most important external factors are temperature, availability of humidity, and the availability of a microbiome that can degrade the polymer in addition to environmental conditions, which allow the microorganisms to thrive[39,43,47–49]. Since the ability of the microbiome to degrade polymers can depend on the molecular mass of the polymer, it is of great interest to determine the biodegradability at different molecular weight ranges.

Therefore, we are addressing two issues in our work the relationship between mechanical properties, biodegradation, and molecular mass. First, molecular mass is a determining factor for degradation pathways like mineralisation or disintegration by embrittlement. Depending on the starting molecular weight, the different degradation pathways can be the cause for the observed varying biodegradation rates in the literature. Furthermore, if mineralisation is observed above the threshold of molecular mass determined in this study, this may indicate a microbiome able to degrade high molecular mass PBS. The second issue we are addressing is determining molecular weight ranges in which the mechanical properties and, therefore, the functionality and stability of products are changing with a declining molecular mass during the ongoing biodegradation.

In this work, we degraded PBS tensile bars and granulates to different molecular masses by hydrolysis in hot water to establish a quantitative relationship between molecular weight and tensile properties. We also assessed experimental factors possibly affecting the comparability of laboratory results with the slow degradation in outdoor environments with lower humidity and lower temperatures. CO_2 evolution of PBS in soil has been investigated in order to determine the molecular mass at which mineralisation of PBS and, therefore, the complete conversion to CO_2, water, and biomass is possible and whether this point could influence the mechanical properties. The mechanical properties of PBS with different molecular masses were determined by tensile testing. Ultimately, we identified important molecular mass ranges in which the mechanical and biodegradation behaviours are changing.

Results

Stress-strain behaviour

The stress-strain curves observed during tensile testing of the different degraded molecular weights can be grouped into three categories without a clear molecular weight threshold separating them. High molecular weight PBS showed necking behaviour after the yield point. The stress-strain curves for this category (see also Fig. 1a, b) could be observed down to a M_w of 80,446 g/mol. Stress-strain curves for tensile bars between a M_w of 102,406 g/mol and 60,610 g/mol can be attributed to the second category and showed elastic and plastic deformation until fracture occurred after the yield point without necking (Fig. 1c). Below a M_w of 57,693 g/mol, the tensile bars became even more brittle, exhibited lower tensile strengths, and broke after a short elastic deformation (Fig. 1d). As can be seen in Fig. 1b, tensile bars of the same molecular weight can behave differently during tensile testing, presumably due to inhomogeneities and defects. Necking often occurred for high molecular weight PBS. After the yield point, necking began and moved along the tensile bar on one side of the necking area. This can be observed in the stress-strain curves (see Fig. 1) as strain softening. The stress–strain curves were also affected by several effects. When the necking front reached the beginning of the shoulder of the tensile bars, it began moving instead on the other side of the necking area with the lower cross-sectional area. Afterwards, for barely degraded PBS, sometimes it also moved inside the first and later the second shoulder of the tensile bars, at some point leading to a small jump of the contact gauges. In these cases, the effect on elongation at break was, in our assessment, small enough to let the tensile test continue.

Mechanical properties

We evaluated several mechanical properties accessible by tensile testing with M_w ranging from 41,947 ± 261 g/mol to 133,667 ± 702 g/mol. The Young's modulus describes the resistance of the material against elastic deformation, the tensile strength is the maximum stress the material could withstand, and the elongation at break is a good indicator of embrittlement. These properties show different dependencies on molecular mass, as shown in Fig. 2. Young's modulus kept rising while molecular mass was degrading. The decrease of tensile strength even accelerated with lower molecular mass below a M_w of 60,000 g/mol. Elongation at break declined fast with decreasing molecular mass at higher molecular masses and then slowed down at lower molecular masses. Elongation at break decreased rapidly between 80,000 g/mol and 110,000 g/mol. Below 40,000 g/mol, it was not possible to test or prepare tensile bars regardless of the preparation method because the material had become too brittle. Tensile bars degraded at 115 °C exhibit a higher Young's modulus and tensile strength but lower elongation at break than other tensile bars of similar molecular mass and an increased

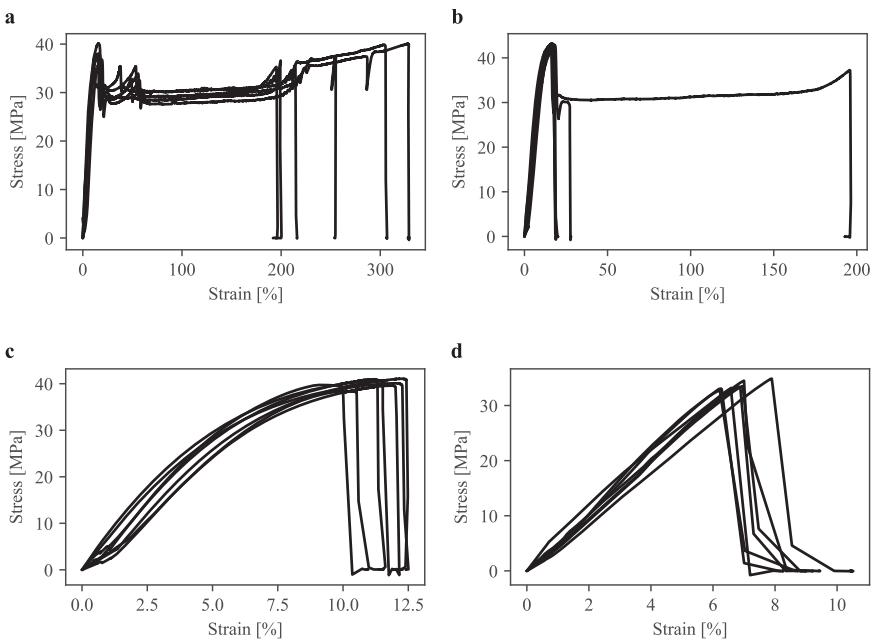

Fig. 1 | Stress-strain curves. Stress-strain curves exhibiting typical behaviour for different molecular weight ranges. **a** M_w of 105,833 g/mol: High molecular weight PBS shows necking behaviour, including strain-softening and strain-hardening. The necking front jumps several times from one side of the neck to the other. **b** M_w of 107,166 g/mol: Sometimes, necking behaviour is not observed for some tensile bars despite the high molecular weight. **c** M_w of 80,530 g/mol: No necking could be observed for medium molecular weights, but a significant plastic deformation occurred after the elastic deformation. **d** M_w of 57,693 g/mol: Tensile bars of low molecular weight were very brittle and broke after elastic deformation with a lower tensile strength. There was no clear molecular weight threshold between the categories, as can be seen in the example of **b**.

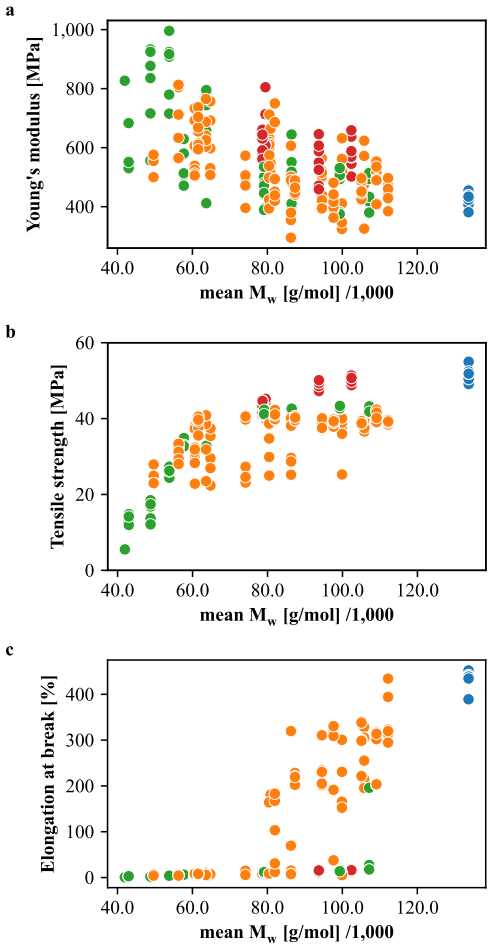

Fig. 2 | Mechanical properties versus molecular mass. Data points for the relationship of the molecular mass to Young's modulus (**a**), tensile strength (**b**), and elongation at break (**c**) are shown. Blue dots: non-degraded tensile bars, orange dots: tensile bars made from degraded granulates, green dots: at 60 °C degraded tensile bars, red dots: at 115 °C degraded tensile bars. Fitted models and their parameters are provided in the Supplementary Figs. 1–7.

crystallinity. A comparison of different available mathematical models with their respective parameters is provided in Supplementary Note 1 and Supplementary Fig. 1–7.

Influence of degradation on tensile bars

Beginning with industrially available high molecular weight PBS granulates, we degraded them to lower molecular weights for our study. Since accelerated hydrolysis at higher temperature may change important factors affecting tensile properties, we analysed the samples to validate the comparability of the data. Regardless of the degradation pathway, tensile bars showed the same cross-sectional area. Tensile bars from degraded and non-degraded granulate had a cross-sectional area of 9.99 ± 0.12 mm^2, whereas tensile bars, which had been degraded at 60 °C or 115 °C had a cross-sectional area of 10.01 ± 0.13 mm^2 and 9.95 ± 0.16 mm^2 respectively. The crystalline fraction of the polymer did not change with degrading molecular mass as determined by X-ray diffractometry (XRD) (see Supplementary Fig. 9). Tensile bars from non-degraded granulates had a crystalline fraction of 0.55 ± 0.02, at 60 °C degraded tensile bars 0.62 ± 0.04 and tensile bars from degraded granulates 0.59 ± 0.04. The degradation at higher temperatures led to further crystallisation up to a crystalline fraction of 0.69 ± 0.02. As shown in Fig. 3, the grain volume of the crystallites is rising with degrading molecular mass. The trend seems to hold for all degradation types but for the tensile bars, which were degraded at 115 °C. They showed a higher grain volume than tensile bars degraded to the same molecular mass at a lower

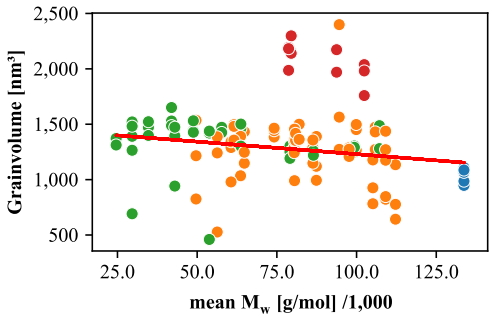

Fig. 3 | Grain volume versus molecular weight. The grain volumes of the crystallites determined by XRD are plotted against M_w and a fit for the linear decrease with increasing molecular mass with a Pearson correlation coefficient of −0.25 is shown (slope = −0.002, intercept = 1456, R^2 = 0.06). Values for tensile bars that have been degraded at 115 °C are shown but not included in the fit. Blue dots: non-degraded tensile bars, orange dots: tensile bars made from degraded granulates, green dots: at 60 °C degraded tensile bars, red dots: at 115 °C degraded tensile bars.

temperature or made from degraded granulates. The rise of the grain volume was driven by an enlargement of the crystal in the direction of the c-axis with a correlation coefficient of −0.42 and in the direction of the a-axis with a correlation coefficient of −0.27, whereas 010 only showed a slight increase with a correlation coefficient of −0.12 for increasing molecular mass.

Influence of degradation on the crystallinity of powdered PBS for biodegradation

The crystalline content of the powdered degraded PBS granulates for the biodegradation experiment had been analysed by differential scanning calorimetry (DSC). No trend with degrading molecular mass was found as shown in Supplementary Fig. 10. However, the degradation temperature mattered: PBS degraded at 60 °C yielded a crystalline fraction of 0.49 ± 0.05, whereas the PBS with the lowest M_w of 8060 g/mol, which had been hydrolysed in hot water at temperatures above 100 °C exhibited a crystalline fraction of 0.67 ± 0.01.

Biodegradation

CO_2 is commonly accepted as the only degradation product (except the corresponding oxygen demand) which can be attributed with certainty to the digestion of the sample by microorganisms[34,50,51]. In the following, the amount of carbon actually metabolised to CO_2 divided by the theoretically amount of CO_2 evolved by a completely metabolised sample is referred to as "biodegradation". The only sample showing a significant biodegradation in soil was the one with the lowest M_w of 8060 g/mol, which reached a cumulative biodegradation of 5.18 ± 0.34% after 38 days and 6.46 ± 0.58% after 92 days as shown in Fig. 4. The next sample with a slightly higher molecular mass of 26,666 g/mol achieved a cumulative biodegradation of 1.16 ± 0.37% after 38 days and 1.78 ± 0.68% after 92 days. The same sample was also investigated in a smaller grain size below 125 micrometre and yielded a slightly higher biodegradation of 1.20 ± 0.78% after 38 days and 2.57 ± 0.65% after 92 days. The biodegradation of both grain sizes is higher but still similar to all other PBS samples with a higher molecular mass, which have been mineralised between 0.13 ± 0.28% and 1.04 ± 0.72% after 38 days and 0.22 ± 0.44% and 1.66 ± 0.10% after 92 days. In comparison, cellulose as positive control for a microbial-active and degrading environment, reached a cumulative biodegradation of 65.74 ± 2.76%. In contrast, PP as negative control for possible effects of addition of non-biodegradable material to the soil showed a cumulative biodegradation of 2.48 ± 0.36% after 92 days. Therefore, the low biodegradation of PBS with a higher M_w may not be caused by its biodegradation. While dispersity of the samples did not change for the hydrolysed samples above 32,000 g/mol with a dispersity of 1.73 ± 0.08, the samples with a M_w of 26,667 g/mol and 8060 g/mol were determined with a dispersity of 2.76 ± 0.30 and 2.81 ± 0.40, respectively.

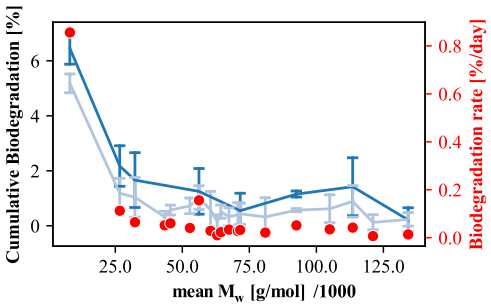

Fig. 4 | Mineralisation versus molecular mass. The cumulative biodegradation dependency on M_w is shown after 38 days (light blue) and 92 days (dark blue), as well as the highest biodegradation rate per day over the course of the experiment(red dots). The standard deviation is shown by error bars.

This means that PBS hydrolysed to low molecular weights with a broader molecular weight distribution is biodegradable.

Discussion

The transition from abiotic to biotic degradation is important for the environmental degradation of polymers. Nearly no biodegradation was observed for most of the molecular mass samples of PBS during 92 days. Between a M_w of 8060 g/mol and 26,666 g/mol, there appears to be a critical molecular mass below which microorganisms can mineralise the polymer chains to CO_2. The real threshold molecular mass for single chains may be even lower since the sample of 8060 g/mol reached a cumulative biodegradation of only 6.46 ± 0.58% after 92 days which is similar to the fraction of the sample of 6.9 ± 1.3% that has a molecular mass below 1000 g/mol and can be assumed to be water soluble and readily biodegradable[52]. This observation is contrary to results reported by other authors who found that PBS with a M_w of 56,000 g/mol were successfully mineralised in soil[4]. These differences are typical for PBS. Two other studies also found inconsistent results for biodegradation in different soils. At 19 different sites, PBS was degraded between 1.6% and 100% within 12 months. In three of the 19 soils, PBS showed a complete degradation, in two a degradation above 50%, in 5 more than 25% and in 7 soils degradation was below 10%, which gives an impression of the distribution of soil capability to degrade PBS[39]. In another investigation, 46% weight loss of PBS was found in one soil but no degradation in another at the same temperature. Differences in the respective microbiome of the soils could explain this discrepancy[53]. This leads to the conclusion that the soil used in our study does not contain a suitable microbiome for the degradation of high molecular weight PBS and biotic and that the identified threshold molecular weight for biodegradation is valid for soils with corresponding microbiomes. Since mechanical properties are lost well above the threshold for significant biodegradation, one has to consider only factors regarding hydrolysis as the predominant degradation mechanism in soil for modelling changes in the functionality of a product made from PBS. Samples showed a higher biodegradation rate if the particle size was lower, resulting in an increased surface area. While it was surprising to see this effect even for low biodegradation rates, it is well-known in the literature for the biodegradation of PLA[37,54].

We have also investigated the dependency of mechanical properties like the Young's modulus, the tensile strength and elongation at break on molecular mass. In order to compare results from different studies more easily, we are providing in the following section the estimated corresponding M_n or M_w values in our study in brackets calculated with the average dispersity of 1.86 ± 0.14 observed in our study. The Young's modulus in our study increased with lower molecular masses up to 873 ± 104 MPa. In comparison, Jin et al. observed a maximum of 396.3 ± 3.1 MPa at a M_n of 33,000 g/mol (M_w ≈ 61,380 g/mol) and a decrease towards higher and lower molecular masses for synthesised PBS[31]. We found that the tensile strength was at high molecular masses slowly decreasing with decreasing molecular mass and then dropped faster below a M_w of 60,000 g/mol (M_n ≈ 32,258 g/mol). This fits well with observations on hydrolysed PBS and PBAT as well as PBS films[32,33]. On the other hand, Jin et al. found a maximum at a M_n of 41,000 g/mol (M_w ≈ 76,260 g/mol) and a decrease for lower and higher M_n.

In our study, elongation at break was still increasing with increasing molecular mass, which fits well with the results from Han et al. and Muthuraj et al. In contrast, Jin et al. found it to decline after a maximum was reached at a M_n of 50,000 g/mol (M_w ≈ 93,000 g/mol)[31–33]. The observation of a maximum with a decline to higher molecular weights in contrast to our results may be explained by the larger deviations of crystallinity of the samples by Jin et al.

The sudden change in elongation at break can be described by a critical molecular mass for the ductile-brittle transition. The critical molecular mass for PET was found to be above a M_n of 17,000 g/mol, for PP between 170,000 g/mol and 250,000 g/mol depending on the degradation pathways photo-oxidation, thermal oxidation or radiochemical oxidation and for PE between 40,000 g/mol and 100,000 g/mol[18,22]. This is the same order of magnitude as for the ductile-brittle transition observed in our study for PBS.

As can be seen in Fig. 2, the measurements of the mechanical properties of degraded PBS show a large variability. One factor for this may be the used equipment. Only one tensile bar could be prepared per injection of the melt into the mould. While care has been taken, usually, bigger injection moulding machines are used and five to ten specimens can be prepared in the same shot with exactly the same temperature and duration in the melt. Furthermore, we fixated the tensile bars in the tensile testing machine manually. Small differences in the angle and the use of a contact strain gauges may also lead to a premature failure of the tensile bars[55] due to a shift in the applied force vector —especially if the behaviour of a degraded sample is prone to inhomogeneities. While tensile bars were checked for defects prior to tensile testing and also afterwards at the fracture surface, it is possible that small changes, defects or inhomogeneities in the distribution of the crystallites and the molecular weight have been introduced by the ageing process, which could not be captured by XRD and visual inspection. Therefore, the variability may be, to some extent, part of the degradation process.

Long-term processes in the environment with many influencing factors are best emulated in the laboratory. Therefore, it is important to check the most important factors which may be affected by the experimental setup. In this study, the polymer was degraded at elevated temperatures in water. While this leads to accelerated hydrolysis, it may also lead to swelling and further sample crystallisation. To reduce the possible effects on the comparability of the laboratory results to the process in the environment, we checked the cross-sectional area of the tensile bars and their crystallinity after the degradation. We also degraded the samples at different temperatures to see if there was any effect of rising temperatures. Finally, we also prepared tensile bars from already degraded polymer granulates because melting should remove any effect introduced by accelerated hydrolysis. We assumed that those tensile bars may be otherwise not comparable to directly degraded samples since crystallinity, surface roughness, and other changes in the microstructure may occur. Nevertheless, we found no influence of the degradation parameters on the cross-sectional area of the tensile bars and, therefore, no swelling. The degradation temperature influenced crystallinity. A degradation at 115 °C led to a higher crystallinity of 0.70 ± 0.04 while at 60 °C degraded tensile bars and tensile bars from degraded granulates had a similar crystalline content of 0.60 ± 0.04 and 0.62 ± 0.07. Tensile bars from non-degraded high molecular mass PBS had, in comparison, a crystalline content of 0.52 ± 0.07. Therefore, we excluded the tensile bars degraded at 115 °C from the comparison. Since crystallinity and cross-sectional area did not differ much for samples prepared by the different degradation parameters, we conclude that our results for tensile bars prepared by different parameters, except those at 115 °C, are comparable to outdoor degradation processes at lower temperatures.

We assumed that during the degradation of PBS, specific molecular mass thresholds exist for the mechanical properties and biodegradability. We have found such a critical molecular mass for the mineralisation in soil between a M_w of 8060 g/mol and 26,666 g/mol. The biodegradation corresponds to the content of water-soluble polymer chains below 1000 g/mol.

This contradicts other studies, which observed mineralisation of high molecular mass PBS in soil. Mechanical properties changed over a larger molecular mass range, but below a critical M_w of 40,000 g/mol, no mechanical properties could be measured any more. Embrittlement by hydrolysis occurs between a M_w of 80,000 g/mol and 110,000 g/mol, a fast decline of tensile strength was observed below 60,000 g/mol. In contrast, the Young's modulus kept increasing with decreasing molecular mass which is contradictory to some literature reports on synthesised PBS. Knowing the dependency of biodegradability on the molecular mass allows for determining the relevant degradation pathways and their most important parameters. Without soil containing a microbiome able to degrade high molecular mass PBS, abiotic hydrolysis can be expected to be the predominant degradation mechanism for polymers of high molecular mass. Below the embrittlement criteria, weight loss and microplastic formation may occur. The dependency of mechanical properties on molecular mass is essential for selecting materials suitable for recycling or for products with an intended service time frame. Combined with a kinetic model for the biodegradation of PBS, it is possible to predict the service life of products in degrading environments and the time of mechanical failure. Our results are also crucial for monitoring the functionality of products made from PBS for use in the environment. Our results are valid for soils without a microbiome, which can degrade high molecular mass PBS, and for hydrolytically degraded samples. The mechanical properties of PBS degraded by other degradation pathways or freshly synthesised may behave differently. The development of robust biodegradation models for different degrading environments and a more simple method to discern, for example, soils with a microbiome capable of degrading high molecular mass PBS from those without this capability are needed for a more widespread use of biodegradable products for environmental and biomedical applications.

Methods

Degradation of molecular mass

In order to attain different molecular masses for mechanical properties, PBS granulates (grade FZ71, PTT MCC Biochem, Bangkok, Thailand) were degraded between temperatures of 60 °C and 135 °C. Since crystallinity was affected by temperatures above 60 °C, we varied the hydrolysis time for granulates degraded at 60 °C between a few days and a few weeks, depending on the desired molecular weight. Granulates degraded at higher temperatures were melted before further use in order to remove changes to crystallinity. Since polymers with lower molecular masses could not be injection moulded, some tensile bars made from not yet degraded PBS were directly degraded at 60 °C. At this temperature, the influence of degradation on swelling and the crystalline fraction was negligible in contrast to the degradation of tensile bars at 115 °C. All tensile bars were air dried and stored in a box with a beaker with a saturated $MgCl_2$ solution to set air humidity to 30%. For the biodegradation experiment, granulates degraded at 60 °C were dried, then frozen in N_2(l) and mixed with an A 11 basic analytical mill (IKA-Werke GmbH & CO. KG, Staufen, Germany) with an A 11.3 Beater. Samples were then sieved through 2 mm, 1 mm, 500 micrometre, and 125 micrometre meshes to yield different grain size fractions.

Determination of molecular mass by SEC

The molecular mass was determined by size exclusion chromatography (SECcurity GPC System, PSS, Mainz, Germany) with a set of SDV 5 µm columns containing a pre-column, a 100,000 Å column, a 1000 Å column, and a refractive index detector (1260 Infinity, Agilent, United States of America). PS standards from 682 g/mol to 526,000 g/mol were used for calibration. Samples were injected at a concentration of 5 g/L in chloroform at a flow rate of 0.7 mL/min. Molecular mass for each set of tensile bars was determined from three tensile bars, while for the biodegradation experiment, one powdered and, therefore, representative sample was injected three times into the SEC.

Preparation of tensile bars

Tensile bars were prepared by injection moulding (Haake MiniJet Pro, Thermo Fisher Scientific) of PBS granulates after 15 minutes of melting between 125 °C and 135 °C and with applied pressures between 100 bar and 300 bar for 15 seconds. We designed a three-part injection mould for tensile bars of type 1BA based on DIN EN ISO 527 to allow a more gentle removal of the tensile bar than in the original two-part injection mould[56]. The design is shown in Supplementary Fig. 8. It allowed us to produce tensile bars down to a M_w of 41,947 g/mol with the side effect of flashes that barely changed material properties as tested on non-degraded PBS.

Determination of crystallinity by DSC

Small particles from the crushed fractions were analysed by differential scanning calorimetry. 5 mg to 15 mg of samples were heated in a DSC (DSC 1 Stare System, Mettler Toledo, Columbus, Ohio, United States of America) from 25 °C to 250 °C with 10 °C/min. Crystalline content was calculated by the following equation (1)

$$x_c = \frac{\Delta H_m - \Delta H_{cc}}{H_m^0} \quad (1)$$

with ΔH_m being the observed melting enthalpy of the sample, ΔH_{cc} the observed cold crystallisation enthalpy and ΔH_m^0 being the melting enthalpy for 100% crystalline PBS. We used the ΔH_m^0 determined on extended-chain crystals with 133.5 ± 3 J/g.[57].

Determination of crystallinity by XRD

We analysed changes in the crystalline content of the tensile bars after tensile testing by XRD (MiniFlex 600, Rigaku, Tokyo, Japan) with a copper anode and a silicium strip detector (D/teX Ultra, Rigaku) from 10° to 80° in 0.02° steps at a scan speed of 5° per minute. For each molecular mass, the top parts of three tensile bars were analysed. After Rietveld-refinement with the software BGMN (version 4.2.23), the crystallinities were calculated according to Ruland and Vonk[58–60]. Atomic coordinates for PBS-α phase were taken from Ichikawa et al.[61].

Tensile testing

A universal tensile testing machine (smarTens 010, Karg Industrietechnik, Krailling, Germany) was used to determine the mechanical properties. For the measurement of elongation, contact displacement transducers were used. To correct for the influence of tensile bar mounting, all tensile bars were pulled with 1 mm/min until an initial load of 1 MPa. After 1 MPa was reached, samples were pulled with 5 MPa/min until an elongation of 0.5% was reached and then with 10 mm/min until the measured stress fell below 75% of the maximum of the recorded stress. This indicated that fracture occurred, and elongation at break was determined. The maxima of the stress-strain curve yielded the tensile strength, Young's moduli were evaluated at the elastic deformation region and work of fracture was determined as the integral of the stress-strain curve. We also investigated several mathematical models describing the relationship between molecular weight and mechanical properties. Models were fitted via Python and the *optimise.curve_fit* algorithm using non-linear least squares and *stats.linregress* using linear least squares regression from the *scipy* package version 1.3.3[62]. Further details and results are available in Supplementary Note 1.

Biodegradation

Biodegradation of samples was determined by quantifying the evolving CO_2 during mineralisation of the samples compared with the background CO_2 of soil without samples. The evolved CO_2 was absorbed in 20 mL of a 1 mol/L KOH solution and then titrated with 0.6 mol/L HCl. The amount of CO_2 corresponds to the volume of HCl between the two inflection points of the pH-titration curve at a pH of 8.1 and 3.9. The KOH solutions were titrated and replaced every 2–27 days, when the pH approached 9 to ensure a quantitative CO_2-absorption. Before the biodegradation experiment started, we acquired a soil containing 50% compost and 50% topsoil from the local composting facility (Zweckverband Abfallwirtschaft Straubing Stadt und Land, Straubing, Germany). The manufacturer described it as loamy, humous soil. In order to remove organic residues, the soil was sieved through

a 1 mm mesh. The soil should be as wet as possible but not muddy in order to yield a microbial-active biodegradation environment while keeping the biodegradation process aerobic and allowing a proper evolvement of the produced CO_2. Therefore, water content was increased until the expectations were met at 0.209 g/g water/dried soil. 300 g soil and a custom-made metal structure for placing the beakers containing the KOH solution in the air without soil contact were placed in each 3-L-jar. Equal background production of each jar was determined before adding 3 g of the sample with a particle size below 500 micrometre. Each molecular weight fraction of PBS was determined in triplicate from 8060 g/mol to 134,000 g/mol. Cellulose powder (α-cellulose, Sigma-Aldrich, St. Louis, Missouri, United States of America) was used in four jars as a positive control, and PP in three jars as a negative control. Four jars with soil but without samples were used as a reference for the CO_2 background. The biodegradation of each sample was calculated by subtracting the mean weight of CO_2 of all blanks from every jar and then dividing the net CO_2 of the sample by the theoretically possible amount of CO_2 evolution after complete biodegradation. The carbon contents of the samples were determined in triplicate by elemental analysis (Euro EA Elemental Analyzer, Euro Vector S.P.A., Italy). The biodegradation experiment was carried out over 92 days with room temperature set to 23 °C. We reduced the number of investigated molecular mass fractions after 38 days due to the lack of biodegradation and, therefore, useful information.

Data availability

The datasets used and analysed during the current study are available from the corresponding author upon reasonable request.

Received: 3 April 2024; Accepted: 8 September 2024;
Published online: 17 September 2024

References

1. Global polybutylene succinate (PBS) market – industry trends and forecast to 2029. Tech. Rep., Databridge Market Research Private Limited, 411028 Maharashtra, India (2022).
2. Mtibe, A. et al. Recent insight into the biomedical applications of polybutylene succinate and polybutylene succinate-based materials. *Express Polym. Lett.* **17**, 2–28 (2023).
3. Barletta, M. et al. Poly(butylene succinate) (PBS): Materials, processing, and industrial applications. *Prog. Polym. Sci.* **132**, 101579 (2022).
4. Nelson, T. F. et al. Biodegradation of poly(butylene succinate) in soil laboratory incubations assessed by stable carbon isotope labelling. *Nat. Commun.* **13**, 5691 (2022).
5. Pliquet, M. et al. Multiscale analysis of the thermal degradation of polyamide 6,6: correlating chemical structure to mechanical properties. *Polym. Degrad. Stab.* **185**, 109496 (2021).
6. Hakkarainen, M. & Albertsson, A.-C. Indicator products: a new tool for lifetime prediction of polymeric materials. *Biomacromolecules* **6**, 775–779 (2005).
7. Chandra, G. & Pandey, A. Biodegradable bone implants in orthopedic applications: a review. *Biocybern. Biomed. Eng.* **40**, 596–610 (2020).
8. Claes, L. Mechanical characterization of biodegradable implants. *Clin. Mater.* **10**, 41–46 (1992).
9. Fuoco, T., Mathisen, T. & Finne-Wistrand, A. Minimizing the time gap between service lifetime and complete resorption of degradable melt-spun multifilament fibers. *Polym. Degrad. Stab.* **163**, 43–51 (2019).
10. Agarwal, S. Biodegradable polymers: present opportunities and challenges in providing a microplastic-free environment. *Macromol. Chem. Phys.* **221**, 2000017 (2020).
11. Ramalingam, R., Hemath, M., Rangappa, S. M., Siengchin, S. & Chellapandi, P. S. D. Aging effects on free vibration and damping characteristics of polymer-based biocomposites: a review. *Polym. Compos.* **43**, 3890–3901 (2022).
12. Nakano, N. & Hasegawa, S. Effect of molecular weight on tensile strength of polystyrene. *J. Soc. Mater.* **33**, 1206–1212 (1984).
13. Bersted, B. H. & Anderson, T. G. Influence of molecular weight and molecular weight distribution on the tensile properties of amorphous polymers. *J. Appl. Polym. Sci.* **39**, 499–514 (1990).
14. Dobkowski, Z. Determination of critical molecular weight for entangled macromolecules using the tensile strength data. *Rheol. Acta* **34**, 578–585 (1995).
15. Flory, P. J. Tensile strength in relation to molecular weight of high polymers. *J. Am. Chem. Soc.* **67**, 2048–2050 (1945).
16. Martin, J. R., Johnson, J. F. & Cooper, A. R. Mechanical properties of polymers: the influence of molecular weight and molecular weight distribution. *J. Macromol. Sci. Part C.* **8**, 57–199 (1972).
17. Ogawa, T. Effects of molecular weight on mechanical properties of polypropylene. *J. Appl. Polym. Sci.* **44**, 1869–1871 (1992).
18. Fayolle, B., Audouin, L. & Verdu, J. A critical molar mass separating the ductile and brittle regimes as revealed by thermal oxidation in polypropylene. *Polymer* **45**, 4323–4330 (2004).
19. Liu, H. et al. Influence of molecular weight on molding efficiency and properties of sintered UHMWPE thick-size products. *J. Polym. Res.* **28**, 323 (2021).
20. Arhant, M., Le Gall, M., Le Gac, P.-Y. & Davies, P. Impact of hydrolytic degradation on mechanical properties of PET - towards an understanding of microplastics formation. *Polym. Degrad. Stab.* **161**, 175–182 (2019).
21. Hamid, S. H. & Amin, M. B. Lifetime prediction of polymers. *J. Appl. Polym. Sci.* **55**, 1385–1394 (1995).
22. Fayolle, B., Richaud, E., Colin, X. & Verdu, J. Review: degradation-induced embrittlement in semi-crystalline polymers having their amorphous phase in rubbery state. *J. Mater. Sci.* **43**, 6999–7012 (2008).
23. Nunes, R. W., Martin, J. R. & Johnson, J. F. Influence of molecular weight and molecular weight distribution on mechanical properties of polymers. *Polym. Eng. Sci.* **22**, 205–228 (1982).
24. Gleadall, A. C. Modelling degradation of biodegradable polymers and their mechanical properties. Ph.D. thesis, University of Leicester, Leicester (2015).
25. Jiang, N., Yu, T. & Li, Y. Effect of hydrothermal aging on injection molded short jute fiber reinforced poly(lactic acid) (PLA) composites. *J. Polym. Environ.* **26**, 3176–3186 (2018).
26. Tsuji, H. Autocatalytic hydrolysis of amorphous-made polylactides: effects of l-lactide content, tacticity, and enantiomeric polymer blending. *Polymer* **43**, 1789–1796 (2002).
27. Wang, Y., Han, X., Pan, J. & Sinka, C. An entropy spring model for the Young's modulus change of biodegradable polymers during biodegradation. *J. Mech. Behav. Biomed. Mater.* **3**, 14–21 (2010).
28. Moetazedian, A. et al. Mechanical performance of 3D printed polylactide during degradation. *Addit. Manuf.* **38**, 101764 (2021).
29. Vieira, A. F. C., Da Silva, E. H. P. & Ribeiro, M. L. Numerical approach to simulate the mechanical behavior of biodegradable polymers during erosion. *Polymers* **15**, 1979 (2023).
30. Hill, A. & Ronan, W. A kinetic scission model for molecular weight evolution in bioresorbable polymers. *Polym. Eng. Sci.* **62**, 3611–3630 (2022).
31. Jin, T.-x et al. Effect of molecular weight on the properties of poly(butylene succinate). *Chin. J. Polym. Sci.* **32**, 953–960 (2014).
32. Han, Y.-K., Kim, S.-R. & Kim, J. Preparation and characterization of high molecular weight poly(butylene succinate). *Macromol. Res.* **10**, 108–114 (2002).
33. Muthuraj, R., Misra, M. & Mohanty, A. Hydrolytic degradation of biodegradable polyesters under simulated environmental conditions. *J. Appl. Polym. Sci.* **132**, 42189 (2015).
34. Müller, R.-J. Biodegradability of polymers: regulations and methods for testing (Wiley-VCH Verlag GmbH & Co. KGaA, 2005).
35. Torres, A., Li, S. M., Roussos, S. & Vert, M. Poly(lactic acid) degradation in soil or under controlled conditions. *J. Appl. Polym. Sci.* **62**, 2295–2302 (1996).
36. Karamanlioglu, M. & Robson, G. D. The influence of biotic and abiotic factors on the rate of degradation of poly(lactic) acid (PLA) coupons

buried in compost and soil. *Polym. Degrad. Stab.* **98**, 2063–2071 (2013).
37. Husárová, L. et al. Identification of important abiotic and biotic factors in the biodegradation of poly(l-lactic acid). *Int. J. Biol. Macromol.* **71**, 155–162 (2014).
38. Huang, Z. et al. Biodegradability studies of poly(butylene succinate) composites filled with sugarcane rind fiber. *Polym. Test.* **66**, 319–326 (2018).
39. Hoshino, A. et al. Influence of weather conditions and soil properties on degradation of biodegradable plastics in soil. *Soil Sci. Plant Nutr.* **47**, 35–43 (2001).
40. Adhikari, D. et al. Degradation of bioplastics in soil and their degradation effects on environmental microorganisms. *J. Agric. Chem. Environ.* **05**, 23–34 (2016).
41. Zhao, J.-H. et al. Biodegradation of poly(butylene succinate) in compost. *J. Appl. Polym. Sci.* **97**, 2273–2278 (2005).
42. Chandra, R. Biodegradable polymers. *Prog. Polym. Sci.* **23**, 1273–1335 (1998).
43. Tokiwa, Y., Calabia, B., Ugwu, C. & Aiba, S. Biodegradability of Plastics. *Int. J. Mol. Sci.* **10**, 3722–3742 (2009).
44. Zhou, J. et al. Enhanced mechanical properties and degradability of poly(butylene succinate) and poly(lactic acid) blends. *Iran. Polym. J.* **22**, 267–275 (2013).
45. Stloukal, P. et al. Kinetics and mechanism of the biodegradation of PLA/clay nanocomposites during thermophilic phase of composting process. *Waste Manag.* **42**, 31–40 (2015).
46. Shin, J. S., Yoo, E. S., Im, S. S. & Song, H. H. Structural changes of biodegradable poly(tetramethylene succinate) on hydrolysis. *Korea Polym. J.* **9**, 210–219 (2001).
47. Rittmann, B. E. & McCarty, P. L. Environmental biotechnology: principles and applications. Second edn. (McGraw-Hill, New York, 2020).
48. Alexander, M. Biodegradation: problems of molecular recalcitrance and microbial fallibility. *Adv. Appl. Microbiol.* **7**, 35–80 (1965).
49. Itävaara, M. & Vikman, M. An overview of methods for biodegradability testing of biopolymers and packaging materials. *J. Polym. Environ.* **4**, 29–36 (1996).
50. DIN EN ISO 14855-1:2013-04, Bestimmung der vollständigen aeroben Bioabbaubarkeit von Kunststoff-Materialien unter den Bedingungen kontrollierter Kompostierung Verfahren mittels Analyse des freigesetzten Kohlenstoffdioxides Teil 1: Allgemeines Verfahren (ISO 14855-1:2012)
51. DIN EN ISO 17556:2019-09, Kunststoffe - Bestimmung der vollständigen aeroben Bioabbaubarkeit von Kunststoffen im Boden durch Messung des Sauerstoffbedarfs oder der Menge des entstandenen Kohlendioxids (ISO 17556:2019)
52. Kitakuni, E. et al. Biodegradation of poly(tetramethylene succinate-cotetramethylene abdicate) and poly(tetramethylene succinate) through water-soluble products. *Environ. Toxicol. Chem.* **20**, 941–946 (2001).
53. Kamiya, M., Asakawa, S. & Kimura, M. Molecular analysis of fungal communities of biodegradable plastics in two Japanese soils. *Soil Sci. Plant Nutr.* **53**, 568–574 (2007).
54. Stloukal, P., Koutny, M., Sedlarik, V. & Kucharczyk, P. Biodegradation of high molecular weight polylactic acid. *AIP Conf. Proc.* **1459**, 20–22 (Ischia, Italy, 2012).
55. Goldberg, R. K., Roberts, G. D. & Gilat, A. Implementation of an associative flow rule including hydrostatic stress effects into the high strain rate deformation analysis of polymer matrix composites. *J. Aerosp. Eng.* **18**, 18–27 (2005).
56. DIN EN ISO 527-2:2012-06, Kunststoffe Bestimmung der Zugeigenschaften Teil 2: Prüfbedingungen für Form- und Extrusionsmassen (ISO 527-2:2012)
57. Tian, Y.-P., Wu, T., Meng, X. & Ye, H.-M. Thermodynamic features of extended-chain crystals of poly(butylene succinate) and its random copolymers with adipic acid. *Macromolecules* **55**, 5669–5674 (2022).
58. Ruland, W. X-ray determination of crystallinity and diffuse disorder scattering. *Acta Crystallogr.* **14**, 1180–1185 (1961).
59. Vonk, C. G. Computerization of Ruland's X-ray method for determination of the crystallinity in polymers. *J. Appl. Crystallogr.* **6**, 148–152 (1973).
60. Doebelin, N. & Kleeberg, R. *Profex*: a graphical user interface for the Rietveld refinement program *BGMN*. *J. Appl. Crystallogr.* **48**, 1573–1580 (2015).
61. Ichikawa, Y. et al. Crystal structures of α and β forms of poly(tetramethylene succinate). *Polymer* **41**, 4719–4727 (2000).
62. Virtanen, P. et al. SciPy 1.0: fundamental algorithms for scientific computing in Python. *Nat. Methods* **17**, 261–272 (2020).

Acknowledgements

We thank Biofibre (Altdorf, Germany) for their kind supply of PBS granulates, even if they were not involved in the project consortium. We would also like to thank Atittaya Bredenhöller, who supported the experimental work during her research internship. The study was financed by a grant of the 'Zentrales Innovationsprogramm Mittelstand', Federal Ministry for Economic Affairs and Climate Action, Germany, for the 'SuPer (Sustainable Polymer) Hybrid Turf' project. The funder played no role in the study design, data collection, analysis, and interpretation of data, or the writing of this manuscript.

Author contributions

F.E.: conceptualisation, methodology, investigation, formal analysis, visualisation, writing–original draft; D.V.O.: formal analysis, methodology, writing–review & editing; K.S.S.: investigation, methodology, writing–review & editing; C.Z.: funding acquisition, project administration, supervision, writing–review & editing. All authors read and approved the final manuscript.

Funding

Open Access funding enabled and organized by Projekt DEAL.

Competing interests

The authors declare no competing interests.

Additional information

Supplementary information The online version contains supplementary material available at https://doi.org/10.1038/s41529-024-00512-3.

Correspondence and requests for materials should be addressed to Cordt Zollfrank.